

~~ES 71-71~~  
DOC / ATSC

# NATIONAL HURRICANE RESEARCH PROJECT

RC944  
N39  
NO. 71  
ATSC

REPORT NO. 71

Energy Generation and Flux Processes  
Associated With a Weakening Depression  
Over the Gulf of Mexico

ATMOSPHERIC SCIENCE  
LABORATORY COLLECTION





U. S. DEPARTMENT OF COMMERCE  
Luther H. Hodges, Secretary  
WEATHER BUREAU  
Robert M. White, Chief

NATIONAL HURRICANE RESEARCH PROJECT

REPORT NO. 71

Energy Generation and Flux Processes  
Associated With a Weakening Depression  
Over the Gulf of Mexico

by

M. A. Lateef

Department of Meteorology, Florida State University,  
Tallahassee, Fla.



Washington, D. C.  
June 1964



U18401 0601272

NATIONAL HURRICANE RESEARCH PROJECT REPORTS

Reports by Weather Bureau units, contractors, and cooperators working on the hurricane problem are preprinted in this series to facilitate immediate distribution of the information among the workers and other interested units. As this limited reproduction and distribution in this form do not constitute formal scientific publication, reference to a paper in the series should identify it as a preprinted report.

- No. 1. Objectives and basic design of the NERP. March 1956.
- No. 2. Numerical weather prediction of hurricane motion. July 1956.  
Supplement: Error analysis of prognostic 500-mb. maps made for numerical weather prediction of hurricane motion. March 1957.
- No. 3. Rainfall associated with hurricanes. July 1956.
- No. 4. Some problems involved in the study of storm surges. December 1956.
- No. 5. Survey of meteorological factors pertinent to reduction of loss of life and property in hurricane situations. March 1957.
- No. 6. A mean atmosphere for the West Indies area. May 1957.
- No. 7. An index of tide gages and tide gage records for the Atlantic and Gulf coasts of the United States. May 1957.
- No. 8. Part I. Hurricanes and the sea surface temperature field. Part II. The exchange of energy between the sea and the atmosphere in relation to hurricane behavior. June 1957.
- No. 9. Seasonal variations in the frequency of North Atlantic tropical cyclones related to the general circulation. July 1957.
- No. 10. Estimating central pressure of tropical cyclones from aircraft data. August 1957.
- No. 11. Instrumentation of National Hurricane Research Project aircraft. August 1957.
- No. 12. Studies of hurricane spiral bands as observed on radar. September 1957.
- No. 13. Mean soundings for the hurricane eye. September 1957.
- No. 14. On the maximum intensity of hurricanes. December 1957.
- No. 15. The three-dimensional wind structure around a tropical cyclone. January 1958.
- No. 16. Modification of hurricanes through cloud seeding. May 1958.
- No. 17. Analysis of tropical storm Frieda 1957. A preliminary report. June 1958.
- No. 18. The use of mean layer winds as a hurricane steering mechanism. June 1958.
- No. 19. Further examination of the balance of angular momentum in the mature hurricane. July 1958.
- No. 20. On the energetics of the mature hurricane and other rotating wind systems. July 1958.
- No. 21. Formation of tropical storms related to anomalies of the long-period mean circulation. September 1958.
- No. 22. On production of kinetic energy from condensation heating. October 1958.
- No. 23. Hurricane Audrey storm tide. October 1958.
- No. 24. Details of circulation in the high energy core of hurricane Carrie. November 1958.
- No. 25. Distribution of surface friction in hurricanes. November 1958.
- No. 26. A note on the origin of hurricane radar spiral bands and the echoes which form them. February 1959.
- No. 27. Proceedings of the Board of Review and Conference on Research Progress. March 1959.
- No. 28. A model hurricane plan for a coastal community. March 1959.
- No. 29. Exchange of heat, moisture, and momentum between hurricane Ella (1958) and its environment. April 1959.
- No. 30. Mean soundings for the Gulf of Mexico area. April 1959.
- No. 31. On the dynamics and energy transformations in steady-state hurricanes. August 1959.
- No. 32. An interim hurricane storm surge forecasting guide. August 1959.
- No. 33. Meteorological considerations pertinent to standard project hurricane, Atlantic and Gulf coasts of the United States. November 1959.
- No. 34. Filling and intensity changes in hurricanes over land. November 1959.
- No. 35. Wind and pressure fields in the stratosphere over the West Indies region in August 1958. December 1959.
- No. 36. Climatological aspects of intensity of typhoons. February 1960.
- No. 37. Unrest in the upper stratosphere over the Caribbean Sea during January 1960. April 1960.
- No. 38. On quantitative precipitation forecasting. August 1960.
- No. 39. Surface winds near the center of hurricanes (and other cyclones). September 1960.
- No. 40. On initiation of tropical depressions and convection in a conditionally unstable atmosphere. October 1960.
- No. 41. On the heat balance of the troposphere and water body of the Caribbean Sea. December 1960.
- No. 42. Climatology of 24-hour North Atlantic tropical cyclone movements. January 1961.
- No. 43. Prediction of movements and surface pressures of typhoon centers in the Far East by statistical methods. May 1961.
- No. 44. Marked changes in the characteristics of the eye of intense typhoons between the deepening and filling states. May 1961.
- No. 45. The occurrence of anomalous winds and their significance. June 1961.
- No. 46. Some aspects of hurricane Daisy, 1958. July 1961.
- No. 47. Concerning the mechanics and thermodynamics of the inflow layer of the mature hurricane. September 1961.
- No. 48. On the structure of hurricane Daisy (1958). October 1961.
- No. 49. Some properties of hurricane wind fields as deduced from trajectories. November 1961.
- No. 50. Proceedings of the Second Technical Conference on Hurricanes, June 27-30, 1961, Miami Beach, Fla. March 1962.
- No. 51. Concerning the general vertically averaged hydrodynamic equations with respect to basic storm surge equations. April 1962.
- No. 52. Inventory, use, and availability of NERP meteorological data gathered by aircraft. April 1962.
- No. 53. On the momentum and energy balance of hurricane Helene (1958). April 1962.
- No. 54. On the balance of forces and radial accelerations in hurricanes. June 1962.
- No. 55. Vertical wind profiles in hurricanes. June 1962.
- No. 56. A theoretical analysis of the field of motion in the hurricane boundary layer. June 1962.
- No. 57. On the dynamics of disturbed circulation in the lower mesosphere. August 1962.
- No. 58. Mean sounding data over the western tropical Pacific Ocean during the typhoon season. and Distribution of turbulence and icing in the tropical cyclone. October 1962.
- No. 59. Reconstruction of the surface pressure and wind fields of hurricane Helene. October 1962.
- No. 60. A cloud seeding experiment in hurricane Esther, 1961. November 1962.
- No. 61. Studies on statistical prediction of typhoons. April 1963.
- No. 62. The distribution of liquid water in hurricanes. June 1963.
- No. 63. Some relations between wind and thermal structure of steady state hurricanes. June 1963.
- No. 64. Instability aspects of hurricane genesis. June 1963.
- No. 65. On the evolution of the wind field during the life cycle of tropical cyclones. November 1963.

(Continued on inside back cover)

QC944

.N39

no. 71

ATSL

(Continued from inside front cover)

- No. 66. On the filling of tropical cyclones over land, with particular reference to hurricane Donna of 1960. December 1963.
- No. 67. On the thermal structure of developing tropical cyclones. January 1964.
- No. 68. Criteria for a standard project northeaster for New England north of Cape Cod. March 1964.
- No. 69. A study of hurricane rainbands. March 1964.
- No. 70. Some theoretical results which pertain to the upper-tropospheric vortex trains of the Tropics. April 1964.

RECEIVED  
NOV 10 1964  
FBI - NEW YORK

## CONTENTS

	Page
Abstract .....	1
1. Introduction .....	1
2. The Kinetic Energy Balance Equation .....	2
3. Computational Procedures .....	3
4. Terms in the Kinetic Energy Balance Equation .....	8
5. Production of Kinetic Energy in the Depression and Its Surroundings .....	8
6. General Conclusions .....	9
Acknowledgments .....	10
References .....	10

ENERGY GENERATION AND FLUX PROCESSES ASSOCIATED WITH  
A WEAKENING DEPRESSION OVER THE GULF OF MEXICO

M. A. Lateef

Department of Meteorology, Florida State University,<sup>1</sup> Tallahassee, Fla.

ABSTRACT

The dissipation on September 21, 1963, of a depression over the Gulf of Mexico, has been investigated in terms of kinetic energy transport and generation processes. To evaluate these processes, data provided by research flights at the 800- and 600-mb. levels were used. Results show that the limited atmospheric region under study not only was subject to internal conversion of kinetic to potential and internal energy but also transported kinetic energy to the surrounding atmosphere.

1. INTRODUCTION

In recent years there have been several investigations of the energy and momentum budgets of tropical cyclones. In particular, decay of tropical storm circulation over land has been ascribed to surface friction (Gangopadhyaya and Riehl [1]), or removal of oceanic heat source (Miller [3]), or changes in kinetic energy exchange processes (Yanai [4]). The purpose of this study is to compute some of the processes involved in the loss of kinetic energy and weakening of the circulation of a depression which on September 21, 1963 was over the Gulf of Mexico. This depression was located off Key West on the morning of September 20, 1963. During the next 48 hours it moved northward over the Gulf of Mexico. At 1800 GMT on September 21, the surface center of the depression lay near latitude 28.5°N., longitude 86.5°W. Within the next few hours, the intensity of circulation in the lower troposphere diminished rapidly and by 0600 GMT, September 22, only a trough remained.

Cyclonic circulation was clearly evident from sea level to the 500-mb. surface throughout the life of the depression; a shear line could be identified at the 700 and 500-mb. levels during the weakening stage. As far as could be ascertained from available upper air data, the kinetic energy of the system remained nearly constant during its movement prior to 1800 GMT of September 21, from Key West to the northeastern Gulf of Mexico.

Between 1500 and 2100 GMT, September 21, two research aircraft of the National Hurricane Research Project were flown at 800 mb. and 600 mb. over the eastern Gulf of Mexico and the flight paths covered a region which included a major portion of the depression. Although no further flights were undertaken over the region and the data collected did not cover the entire system, it was felt that the availability of data at these two pressure levels justified

<sup>1</sup> This report was prepared while the author was working at the National Hurricane Research Project under contract arrangement with Florida State University, Tallahassee, Fla.

an investigation of the magnitudes of the terms that enter into the kinetic energy budget. The computed values of the various terms should indicate the relative importance of the physical processes contributing to the rapid loss of kinetic energy of the depression and the adjacent atmosphere.

The analysis area is shown in figure 1.

## 2. THE KINETIC ENERGY BALANCE EQUATION

The scalar product of the horizontal wind  $\mathbf{V}$  and the equation of motion leads to

$$\partial K / \partial t + \nabla \cdot \nabla K + \omega \partial K / \partial p = - \nabla \cdot \nabla \phi + \nabla \cdot \mathbf{F} \quad (1)$$

where  $\omega$  ( $= dp/dt$ ) represents vertical motion,  $K$  ( $= \mathbf{V} \cdot \mathbf{V} / 2$ ) is the kinetic energy per unit mass,  $\phi$  is geopotential, and  $\mathbf{F}$  is the frictional force per unit mass.

If we consider the mass,  $M$ , bounded by the perimeter of the grid and extending from 1000 mb. to 600 mb. in the vertical, integration of (1) over this domain yields

$$\begin{aligned} \partial / \partial t \int_M K dM = & - \frac{1}{g} \iint \nabla \cdot K \mathbf{V} dA dp - \frac{1}{g} \int \partial / \partial p \left( \int_A K \omega dA \right) dp \\ & - \frac{1}{g} \iint \nabla \cdot \phi \mathbf{V} dA dp - \frac{1}{g} \int \frac{\partial}{\partial p} \left( \int_A \phi \omega dA \right) dp - \frac{1}{g} \iint \omega \alpha dA dp + \int_M \nabla \cdot \mathbf{F} dM \end{aligned} \quad (2)$$

where  $A$  is area of the grid and  $\alpha$  is specific volume of air.

The first and second terms on the right side of (2) represent net horizontal and vertical fluxes of existing kinetic energy at the boundaries of the domain, while the third and fourth terms represent boundary generation processes. The fifth, or the  $-\omega \alpha$  term, represents conversion from potential and internal energy to kinetic energy through the ascent of warm air and descent of cold air. The last term represents generation and/or dissipation of kinetic energy by motions of smaller scale than are included in the analysis.

Yanai [4] has shown, in the case of a domain with lateral boundaries but extending from the surface to the top of the atmosphere, that the "value of  $-\omega \alpha$  term is partly canceled with exchange of the mean potential energy." In the case of a domain with finite areal and vertical extent, it can be shown that

$$\overline{\nabla \cdot \phi \mathbf{V}} + \partial / \partial p (\overline{\phi \omega}) = \overline{\nabla \cdot \phi' \mathbf{V}} + \partial / \partial p (\overline{\phi' \omega'}) - \bar{\omega} \bar{\alpha} \quad (3)$$

where  $(\overline{\quad}) = \frac{1}{A} \int (\quad) dA$  and we let  $\phi = \bar{\phi} + \phi'$ ,  $\omega = \bar{\omega} + \omega'$  and  $\alpha = \bar{\alpha} + \alpha'$ .

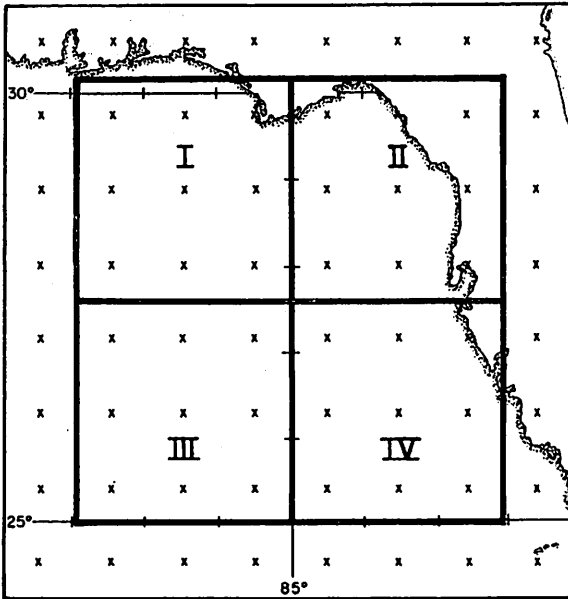


Figure 1. - Base map used for analyses and grid points at which computations have been made. The crosses indicate grid points. The boundaries of blocks are shown in heavy lines.

If we substitute (3) into (2) and apply a two-dimensional form of the divergence theorem, we get

$$\begin{aligned}
 \frac{\partial}{\partial t} \int_M K dM &= - \frac{1}{g} \int_{p_6}^{p_0} \left( \oint_L K v_n dL \right) dp + \frac{1}{g} \left\{ \left( \int_A K \omega dA \right)_{p_6} - \left( \int_A K \omega dA \right)_{p_0} \right\} \\
 &- \frac{1}{g} \int_{p_6}^{p_0} \left( \oint_L \rho' v_n dL \right) dp + \frac{1}{g} \left\{ \left( \int_A \rho' \omega' dA \right)_{p_6} - \left( \int_A \rho' \omega' dA \right)_{p_0} \right\} \\
 &- \frac{1}{g} \int_{p_6}^{p_0} \int_A \omega' \alpha' dA dp + \int_M W \cdot \mathbf{f} dM \quad (4)
 \end{aligned}$$

where  $L$  = perimeter of the grid,

$v_n$  = horizontal wind component perpendicular to the vertical sides, positive outward,

$p_6$  = upper pressure level (600 mb., in our case),

$p_0$  = lower pressure level (1000 mb., in our case).

### 3. COMPUTATIONAL PROCEDURES

The basic data consisted of wind direction and speed, temperature, and geopotential heights at each of the grid points shown in figure 1 for the 1000,

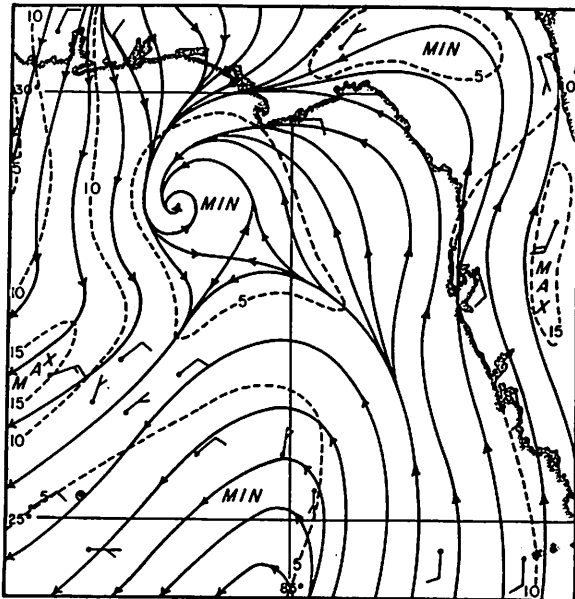


Figure 2. - Streamlines and isotachs (at intervals of 5 kt.) at the 1000-mb. surface, 1800 GMT, September 21, 1963.

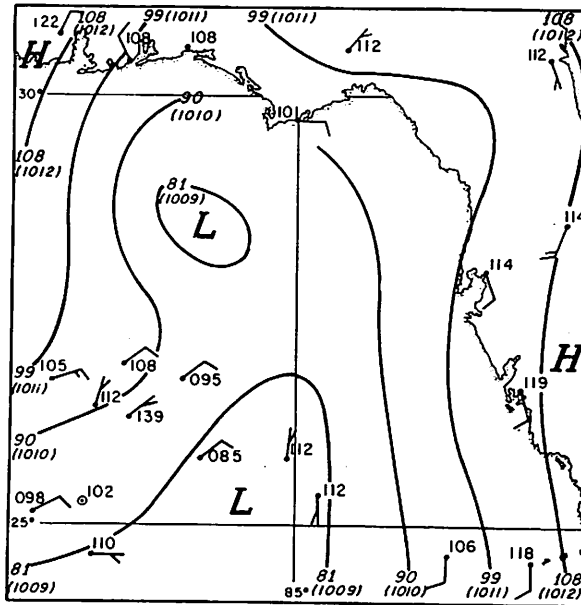


Figure 3. - 1000-mb. geopotential analysis, 1800 GMT, September 21, 1963. Contours are labeled in geopotential meters; corresponding pressure values are shown in parentheses.

800, and 600-mb. levels. Wind data for the 1000-mb. surface were obtained through conventional streamline isotach analysis of 1800 GMT surface observations from ships and coastal stations. Based on the mean height values over the Gulf of Mexico (Hebert and Jordan [2]), the sea level isobars were re-labeled as contours for the 1000-mb. surface. Thus, a sea level pressure of 1012 mb. represented a 1000-mb. geopotential height of 108 m. with increments of 1 mb. in pressure amounting to height changes of 9 m. The wind and height patterns for the 1000-mb. surface are shown in figures 2 and 3. The circulation center and pressure minimum at the surface were located on considerations of continuity of position and intensity as indicated by previous synoptic charts of the District Meteorological Office at Miami.

The height, temperature, and wind data at 800 mb. and 600 mb. were obtained from the aircraft observations as follows. The u and v components, temperatures, and height values observed at 1-min. intervals during the flight were averaged over a flight period of 6 min. and were assigned to the aircraft position at the middle of this period. The average u and v components yielded the average wind direction and speed during the 6 min. For the scale of motions under study, it was not considered necessary to use a shorter smoothing time interval. The height values were, however, adjusted for hydrostatic and gradient wind consistency. Figures 4 to 7 show the wind, height, and temperature patterns at the 800-mb. and 600-mb. pressure surfaces.

The base map used for all analyses was a mercator projection with a scale of  $1:5 \times 10^6$  at  $22.5^\circ\text{N}$ . The values of wind direction and speed, height

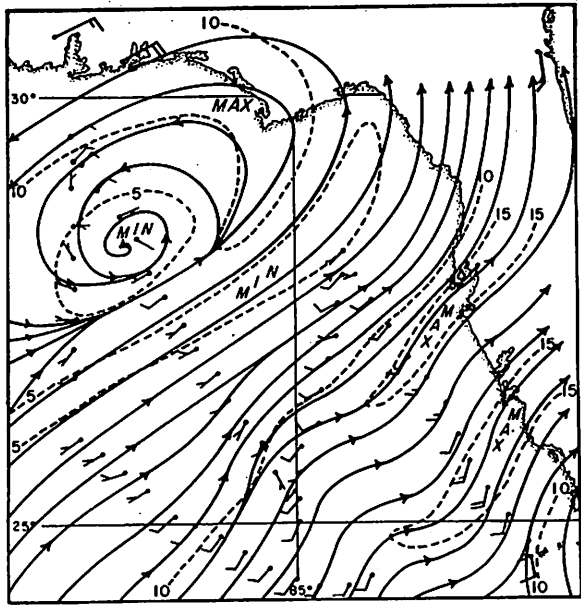


Figure 4. - Streamlines and isotachs (at intervals of 5 kt.) at the 800-mb. surface, 1800 GMT, September 21, 1963.

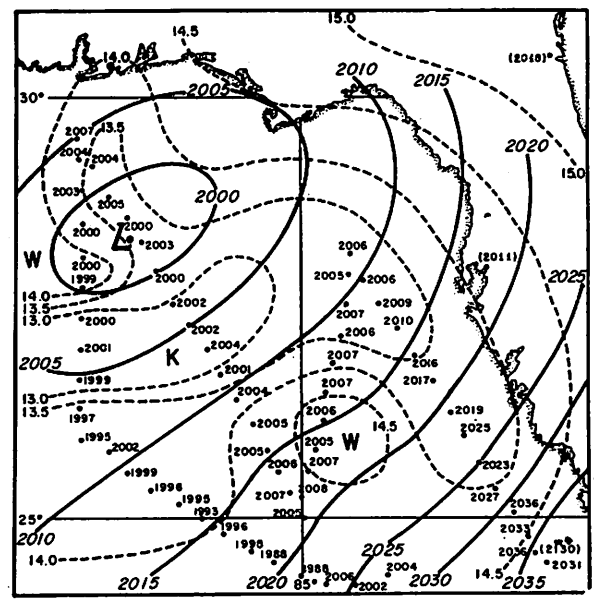


Figure 5. - 800-mb. geopotential and temperature analysis 1800 GMT, September 21, 1963. Contours are labeled in geopotential meters, isotherms are shown by dashed lines labeled in °C.

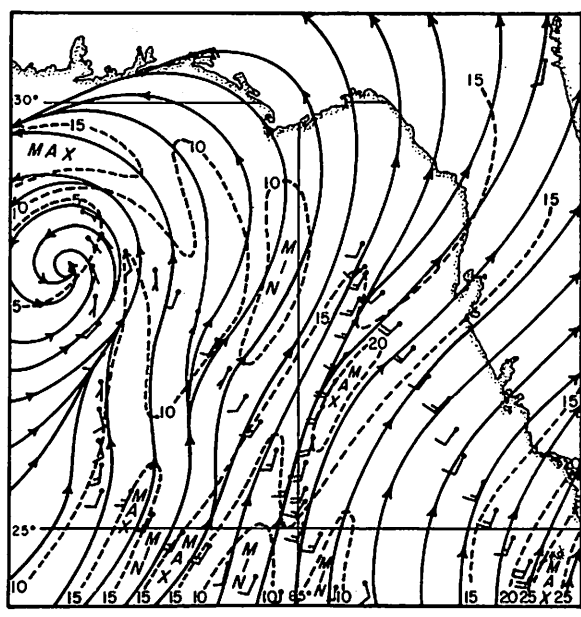


Figure 6. - Streamlines and isotachs (at intervals of 5 kt.) at the 600-mb. surface, 1800 GMT, September 21, 1963.

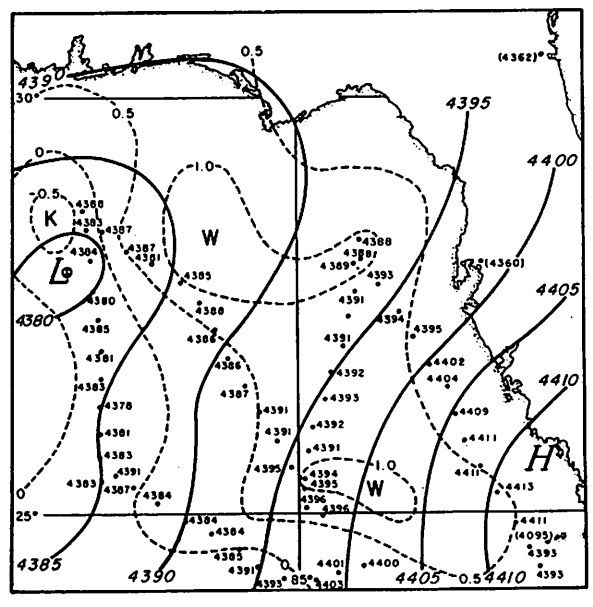


Figure 7. - 600-mb. geopotential and temperature analysis 1800 GMT, September 21, 1963.

and temperature were read over a square array of 64 points (fig. 1) with a grid interval of 96 km.

From the interpolated values of wind direction and speed, the u and v components at the grid points were readily computed. The procedure adopted for computing vertical motion was as follows.

The values of horizontal divergence at the center of each 96-km. square were first computed kinematically. The scheme of computation for a square defined by the grid points (i, j), (i, j + 1), (i + 1, j + 1) and (i + 1, j), with i increasing northward, and j increasing eastward, was

$$D = \frac{1}{2 \times 96 \text{ km.}} [(u_{i,j+1} + u_{i+1,j+1}) + (v_{i+1,j} + v_{i+1,j+1}) - (u_{i,j} + u_{i+1,j}) - (v_{i,j} + v_{i,j+1})] \quad (5)$$

The vertical motion profile at the center of each square was represented as

$$\omega = A \ln \frac{1000}{p} + B \left( \ln \frac{1000}{p} \right)^2 \quad (6)$$

where A and B are parameters which were determined by the divergence values at 800 mb. and 600 mb. Equation (6) implies  $\omega = 0$  at 1000 mb., which is a reasonable lower boundary condition for  $\omega$ . Differentiation of (6) gives

$$D_{800 \text{ mb.}} = \left( - \frac{\partial \omega}{\partial p} \right)_{800 \text{ mb.}} = \left( \frac{A}{p} \right) + \left( \frac{2B}{p} \right) \ln 10/8 \quad (7)$$

$$D_{600 \text{ mb.}} = \left( - \frac{\partial \omega}{\partial p} \right)_{600 \text{ mb.}} = \left( \frac{A}{p_6} \right) + \left( \frac{2B}{p_6} \right) \ln 10/6$$

These two equations when solved simultaneously yielded values for A and B and thus for  $\omega$  as a function of pressure at each of the 49 central grid points (fig. 1). The divergence and vertical motion fields are shown in figures 8 to 11.

Area and line integrals involved in the computation of terms on the right side of (4) were approximated by summations of values representative of area and perimeter increments. Vertical integration was approximated by the trapezoidal rule.

With the above approximations and with input data consisting of wind direction, wind speed, height, and temperature for each grid point, it was possible to compute the terms on the right side of (4), with the exception of the dissipating term. It may be pointed out that the computed values of kinetic energy and flux and generation processes are only appropriate to motions on a scale comparable to the grid interval used.

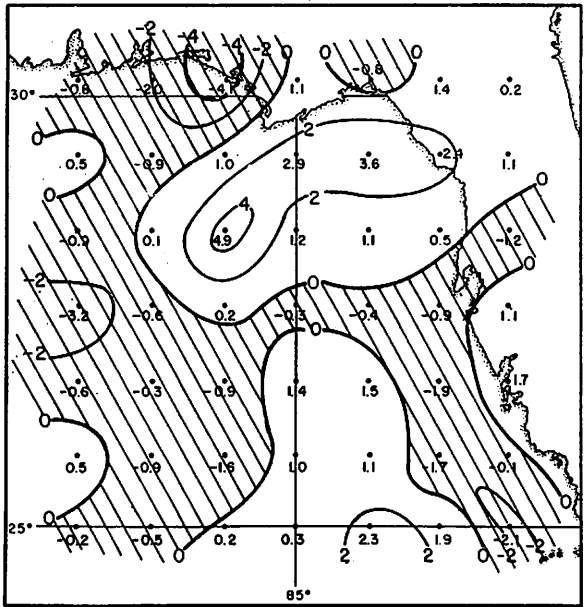


Figure 8. - Horizontal divergence at 800 mb., 1800 GMT, September 21, 1963. Isopleths of divergence values are labeled in units of  $10^{-5} \text{ sec.}^{-1}$ . Shaded areas represent convergence

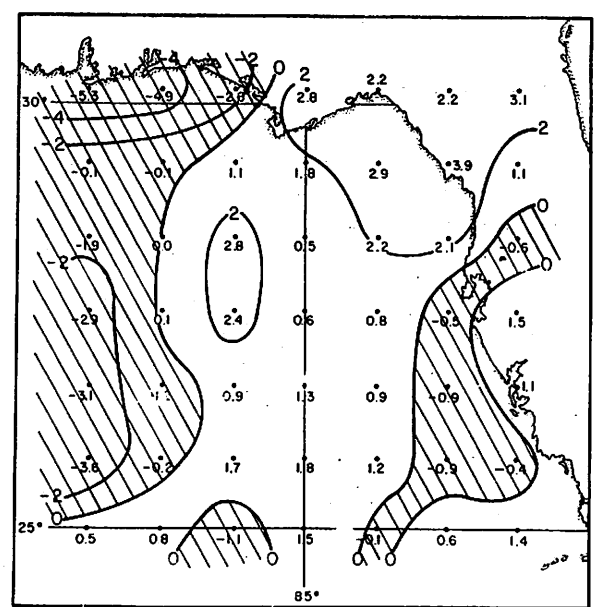


Figure 9. - Horizontal divergence at 600 mb., 1800 GMT, September 21, 1963. Isopleths of divergence values are labeled in units of  $10^{-5} \text{ sec.}^{-1}$ . Shaded areas represent convergence.

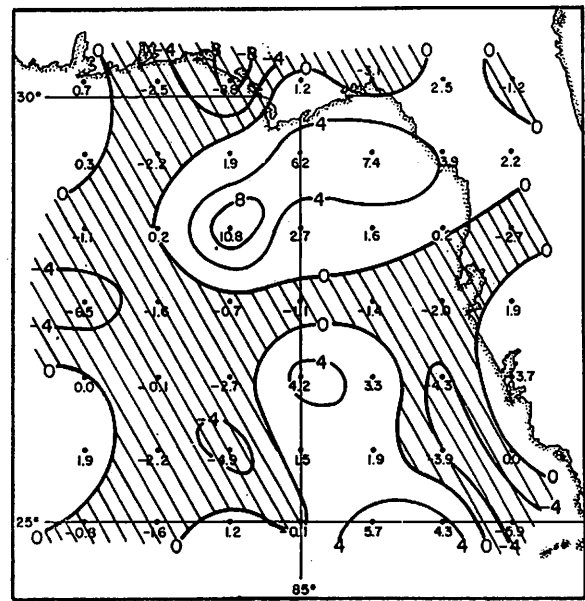


Figure 10. - Vertical motion  $\omega$  at 800 mb. for 1800 GMT, September 21, 1963. Shaded areas represent upward motion. Isopleths are labeled in units of  $10^{-3} \text{ mb. sec.}^{-1}$ , or approximately equivalent to  $1.4 \text{ cm. sec.}^{-1}$

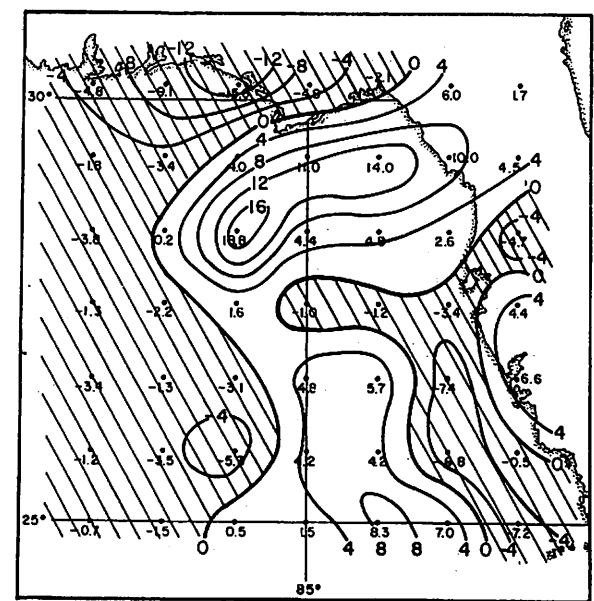


Figure 11. - Vertical motion  $\omega$  at 600 mb. for 1800 GMT, September 21, 1963. Shaded areas represent upward motion. Isopleths are labeled in units of  $10^{-3} \text{ mb. sec.}^{-1}$  or approximately  $1.4 \text{ cm. sec.}^{-1}$

Table 1. - Computed values of terms in the kinetic-energy balance equation, in units of  $10^{18}$  ergs per second. Positive value indicates process acted to increase the kinetic energy of the region.

$(Kv_n)$	$(K\omega)$	$(\phi'v_n)$	$(\phi'\omega')$	$(-\omega\alpha')$
-1.52	0.35	-3.13	2.81	-1.72

#### 4. TERMS IN THE KINETIC ENERGY BALANCE EQUATION

Table 1 gives the values of the computed terms in (4) for the atmospheric region under study.

An immediately obvious feature of these results is the tendency for compensation between the horizontal and vertical fluxes of existing kinetic energy and between the boundary generation processes. The loss of kinetic energy due to conversion to potential energy is apparently not compensated for either by inward transport of kinetic energy through the boundaries or by generation due to the  $\phi'v_n$  or  $\phi'\omega'$  processes. Thus kinetic energy was not only being destroyed within the region but was also being lost to the surrounding atmosphere. The net depletion of kinetic energy due to these flux and conversion processes amounts to  $3.21 \times 10^{18}$  ergs  $\text{sec.}^{-1}$  for the region, or  $622.6$  ergs  $\text{cm.}^{-2} \text{sec.}^{-1}$  for the 1000- to 600-mb. layer. The actual kinetic energy in the region was computed to be  $27.71 \times 10^{22}$  ergs at 1800 GMT. Hence, if only these processes had been operating, kinetic energy of the region would have been reduced to zero in about 24 hours, unless radical changes occurred in some of these processes.

It is more likely that the frictional dissipation action was actually small in the region while certain eddies, not detected on the scale used in the present analysis, produced kinetic energy. The rate of production was not, however, high enough to overcome the loss due to processes on a larger scale. Since the scale of motions included in the present analysis was of the order of 200 km., the eddies which might have produced kinetic energy in the region were perhaps of convective scale.

#### 5. PRODUCTION OF KINETIC ENERGY IN THE DEPRESSION AND ITS SURROUNDINGS

It is of interest to investigate the nature of kinetic energy production in the portion of the region covered by the depression as related to production in other parts of the region. For this purpose, the analysis area was divided into four blocks (fig. 1). Within each block the generation term  $-\mathbf{V} \cdot \nabla\phi$  of (1) was evaluated at each pressure level, using finite differences over the grid intervals. The results given in table 2 show that kinetic energy was generated largely in the surface layer and destroyed in the upper layers. It must be pointed out that since the number of observations at the 1000-mb. level is small, the values of the generation term for this level are likely to contain more uncertainties than those for the higher levels.

Table 2. - Work term ( $-W \cdot \nabla\phi$ ), in units of  $10^{15}$  ergs sec.<sup>-1</sup>

Block	1000 mb.	800 mb.	600 mb.
I	1.76	-0.57	-0.91
II	2.12	-7.09	-3.67
III	-1.32	2.17	0.82
IV	0.94	-2.38	-2.65

As in the case of Blocks II and IV, which incorporate the main stream of southwesterly flow to the east of the depression, kinetic energy was generated in the area of the depression (Block I) in the low levels but was destroyed in the upper levels. In view of the nearly symmetric flow within Block I and the small wind speeds around the depression, it would seem reasonable to neglect energy changes in Block I due to horizontal flux of kinetic energy. Since upward motion was predominant at the 800- and 600-mb. levels over the same area, any contribution due to vertical flux of kinetic energy was certainly negative. Further, the work term ( $-W \cdot \nabla\phi$ ), was such that kinetic energy was destroyed in the upper levels. The small positive rate of generation allowed the kinetic energy in the lower levels to be dissipated easily by frictional stresses at the surface. The depression was thus characterized by a net loss of kinetic energy which could not, perhaps, be overcome by the possible generation of energy by small-scale eddies.

## 6. GENERAL CONCLUSIONS

For the portion of the lower troposphere over the Gulf of Mexico bounded by the 1000- and 600-mb. pressure surfaces, flux and generation terms in the kinetic energy balance equation have been evaluated. Since the region under study was open, energy exchanges with the surrounding atmosphere were considered.

The system was not only subject to internal conversion of kinetic to potential and internal energy but was also acting as a source for the surrounding atmosphere. Such a state presumably resulted from the choice of this particular analysis region which covered only a portion of a short wave. Further, estimates of the so-called frictional term were not possible in the absence of data on actual kinetic energy changes in the region. It is likely that motions on a scale not detected in the present analysis were such that they actually generated kinetic energy.

This study has been based on data at three pressure levels in the lower troposphere and over a limited area at one particular time. The analysis region could not be chosen large enough for computations to be made over the entire extent of the cyclonic flow in the lower troposphere. Moreover, a certain amount of uncertainty in the analyses was inevitable in areas not

actually covered by the aircraft flights. Nevertheless, it is of interest to note that the kinetic energy production rate (represented by the integral of  $-W \cdot \nabla \phi$ ) of  $-1.863 \times 10^{18}$  ergs sec.<sup>-1</sup> compares favorably with the total rate of  $-2.045 \times 10^{18}$  ergs sec.<sup>-1</sup> represented by the sum of the generation terms in table 1. There is need for further studies similar to the current one in order to gain more insight into the processes associated with changes in intensity of cyclones.

#### ACKNOWLEDGMENTS

The author is indebted to Dr. Stanley L. Rosenthal for many helpful discussions throughout the course of this study and wishes to express his appreciation to him and Mr. Harry F. Hawkins for their critical examination of the manuscript. Thanks are extended to Mr. James W. Trout for assistance in programming, to Messrs. Robert Carrodus and Charles True and to Mrs. Bonnie True for their help in preparing the manuscript.

#### REFERENCES

1. M. Gangopadhyaya and H. Riehl, "Exchange of Heat, Moisture, and Momentum between Hurricane Ella (1958) and its Environment," National Hurricane Research Project Report No. 29, U. S. Weather Bureau, 1959, 12 pp.
2. P. J. Hebert and C. L. Jordan, "Mean Soundings for the Gulf of Mexico Area," National Hurricane Research Project Report No. 30, U. S. Weather Bureau, 1959, 10 pp.
3. B. I. Miller, "On the Filling of Tropical Cyclones Over Land," National Hurricane Research Project Report No. 66, U. S. Weather Bureau, 1963, 82 pp.
4. M. Yanai, "On the Changes in Thermal and Wind Structure in a Decaying Typhoon," Journal of Meteorological Society of Japan, vol. 36, No. 4, Aug. 1958, pp. 141-155.